

Magnetic Study of Dilute Magnetic Glasses: [40B₂O₃ + 30Na₂O + (30 - x)V₂O₅ + xFe₂O₃] with x = 0 to 5

P. CHAND* AND L. KUMAR

*Materials Science, Department of Physics, SRM University,
Delhi-NCR Sonapat-131029, Haryana, India*

Received: 15.04.2021 & Accepted: 30.06.2021

Doi: [10.12693/APhysPolA.140.145](https://doi.org/10.12693/APhysPolA.140.145)

*e-mail: satyam20@gmail.com

A magnetic study of dilute magnetic glasses 40B₂O₃ + 30Na₂O + (30 - x)V₂O₅ + xFe₂O₃ with x = 0, . . . , 5 (abbreviated as FVNBx) has been undertaken to understand the effect of magnetic interactions and super-exchange between like and unlike spins. Two complementary experimental techniques were used, namely, the magnetization measurement and the EPR spectroscopy. The study confirmed a minor presence of an active V⁴⁺ oxidation state in the form of a vanadyl (V=O)²⁺ molecular ion. The majority of vanadium remains in the diamagnetic V⁵⁺ oxidation state. It is apparent that vanadium contributes little to the magnetization of these glasses. The experimental value of magnetization of FVNB0 was used to evaluate the concentration of V⁴⁺ and it was found that only 11% of total vanadium transforms to the magnetic V⁴⁺ oxidation state. The magnetization attributed to iron was found also reduced by an order of magnitude from the expected value. The canted antiferromagnetic pairing of the magnetic dipoles is suggested to cause the reduction in the observed magnetization. The effects of magnetic interactions (both dipolar as well as super-exchange) are clearly observed in the EPR spectra of both V⁴⁺ and Fe³⁺ in these glasses. The observed features of EPR are the evidence that iron is experiencing highly distorted oxygen environments (octahedral/tetragonal/tetrahedral) in these glasses, resulting in very high zero field splitting D for the local Fe³⁺ sites. The large D and magnetic exchange interactions between the like and unlike spins are responsible for the complex features of the EPR spectra.

topics: EPR, dilute magnetic glasses, magnetization, iron

1. Introduction

Borate glasses remain attractive for research and applications due to lower temperature fabrication and a variety of chemical compositions for desired properties [1–3]. Gaffar et al. [4] have studied the effect of metal oxides such as V₂O₅, Fe₂O₃, Cr₂O₃, NiO, TiO₂, MnO₂ and CuO on the acoustic properties of alkali borate glasses. Guskos et al. [5] have studied an FeVO₄-Co₃V₂O₈ system by electron paramagnetic resonance (EPR) and DC magnetic susceptibility and found that only 0.58% of all magnetic (Fe³⁺) ions were involved in the ferromagnetic states and the rest were antiferromagnetically coupled. EPR spectra of the samples suggested that the Fe³⁺ high-spin ions coupled by antiferromagnetic (AFM) interaction and clusters of ions play a major role in the observed features of EPR spectra.

Pure soda-borate/silicate/phosphate glasses are diamagnetic in nature. To make glasses magnetic in nature, though, the diamagnetic glasses are modified by adding transition metal ions such as Cu²⁺, Mn²⁺, V⁴⁺, Cr³⁺, Fe³⁺, Co²⁺, Ni²⁺ etc. [6–9].

There are some reports concerning the investigation of the valence states and the distribution mode of the transition metal ions in the network of oxide glasses [10, 11]. The magnetic behavior of the glasses could be meaningfully studied by EPR spectroscopy and complementary magnetization measurements [11]. Despite being more informative, the combined EPR and magnetic susceptibility studies of the magnetic glasses are not frequently done by the researchers. Recently Stefan and Karabulut [12] have studied an Fe₂O₃-P₂O₅-CaO-MgO-B₂O₃ system by X-ray diffraction (XRD), the Fourier transform infrared (FTIR) spectroscopy and EPR and have shown that the structure undergoes changes both in phosphate and iron environments depending upon Fe₂O₃ concentration. The bioactivity tests indicated that an iron-free sample shows some bioactivity but the crystallization tendency increases with increasing iron concentration.

In a previous paper [13], the authors reported magnetic behavior of xFe₂O₃-(2-x)V₂O₅-38Li₂O-60P₂O₅ (x = 0, 1, 2) glasses (abbreviated as FVLPx) containing two magnetic ions, namely,

iron and vanadium in different compositions. The magnetic measurements of FVLP x indicated considerable reduction in the expected magnetization of both vanadium and iron containing glasses. A canted-antiferromagnetic-pairing (CAFMP) of the magnetic ions was envisaged for explaining the reduction of the magnetization in FVLP x glasses. The EPR spectra of FVLP x revealed the presence of a vanadyl ion (V=O)²⁺ and a ferric ion in these glasses. The vanadyl ion was shown to have a distorted octahedral coordination with oxygen to create a tetragonal contraction. The high spin ferric ion in these glasses was concluded to possess two kinds of co-ordinations with oxygen, i.e., rhombic and octahedral. The effects of magnetic exchange (both dipolar as well as super-exchange) on the features of EPR of FVLP x glasses were studied through the number, width, shape, and position of the EPR signals. It was deemed interesting to study the magnetic behavior of the borate glasses containing vanadium and iron in higher concentration as compared to FVLP x glasses. The system Li₂O–P₂O₅ was replaced by Na₂O–B₂O₃. It was expected that P and B atom would have different networks to accommodate iron and vanadium hence the magnetic behavior of the resulting glass network would be different.

A lithium atom was replaced by an Na atom due to the fact that Na has a tendency to bond with vanadium predominantly in the form of diamagnetic NaVO₃ units [14] which, as a consequence, will affect the concentration of magnetic V⁴⁺ oxidation state in the glasses.

The present investigation is aimed at the study of the magnetic behavior of 40B₂O₃ + 30Na₂O + (30 – x)V₂O₅ + x Fe₂O₃ ($x = 0, \dots, 5$) oxide glasses. No indirect approach was made to manipulate the oxidation states of iron and/or vanadium in the glass preparation. It is well known that iron may exist in two oxidation states: Fe(II) ($3d^6$) and/or Fe(III) ($3d^5$) and both of them are strongly magnetic in nature in their high spin states. The magnetic behavior of the materials has been studied by X-band EPR spectroscopy and magnetization measurements by a vibrating sample magnetometer (VSM) [15–19]. Fe(II) is a very fast relaxing ion so the EPR is not observed at room temperature (RT) and can rarely be detected even at liquid helium temperatures. However, Fe(III) is EPR active at RT and even above RT [19]. Vanadium is known to exist in several oxidation states: V²⁺, V³⁺, V⁴⁺ or V⁵⁺ out of which only V⁵⁺ is non-magnetic. The oxidation states V²⁺ and V³⁺ are not common and can only be achieved by special techniques. The oxidation state of V⁴⁺ is very stable and in a wide range of temperature it is EPR active. In the case of V⁴⁺, it can be sensitively identified through its characteristic in the EPR spectrum. Usually, V⁴⁺ bonds with oxygen to form a distinct (V=O) bond known as a vanadyl ion (VO)²⁺ whose EPR is very distinct in solutions,

powders, glasses, and crystals [15]. The presence of magnetic ions in higher concentrations creates exchange and dipolar interactions and consequently alter the magnetic behavior of the glasses. If there are two or more kinds of magnetic ions, then the super-exchange interactions between the like and unlike magnetic ions may further change the magnetic behavior [16, 20]. EPR is a very sensitive tool to monitor the magnetic exchange effects [13, 16]. Therefore it was considered interesting to study the 40B₂O₃ + 30Na₂O + (30 – x)V₂O₅ + x Fe₂O₃ ($x = 0, \dots, 5$) glasses by EPR and VSM. In the present paper, the results of these experimental techniques are presented and discussed.

2. Experimental

2.1. Sample preparation

The magnetic glasses x Fe₂O₃ + (30 – x)V₂O₅ + 30Na₂O + 40B₂O₃ with $x = 0$ to 5 were synthesized by the conventional quick melt-quench technique. The starting materials were analytical grade reagents (ANALR): H₃BO₃ (for B₂O₃), Na₂CO₃ (for Na₂O), V₂O₅ and Fe₂O₃. The desired amounts of components were calculated according to the compositional formula (to be called molar formula henceforth) x Fe₂O₃ – (30 – x)V₂O₅ – 30Na₂O – 40B₂O₃, where $x = 0, 2, 3$ and 5. The calculated stoichiometric amounts of the desired composition were well mixed and homogenized. The homogenized powders were then melted in high purity alumina crucibles at a temperature of 1100 (±25) °C in an electrically heated and temperature-controlled muffle furnace for about 1 h. The alumina crucibles containing glass melts were swirled frequently to insure the homogeneity of the melt. The melts were then quickly quenched to a lower temperature (≈ 300 °C) by pouring onto clean thick stainless steel (SS) plates preheated to 300 °C and subsequently pressing by another thick SS plate which was preheated to about 300 °C to provide a uniform quenching rate and to reduce the quench-induced strains during glass formation. By this method, smooth surfaces of the plate-glass samples were obtained upon cooling ambient to room temperature (RT).

2.2. X-ray diffraction

The as-prepared samples were crushed to fine powders and analysed by an X-ray diffractometer (XRD, Rigaku Ultima IV) by employing Cu K_{α} radiations with nickel filter. The diffraction patterns were obtained for 2θ angle from 20° to 80° at a scan rate of 2° per min. The prepared plate glasses were annealed at 200 °C for several hours to remove any moisture and residual stress. For XRD recording at RT fine powders of the glasses were obtained by crushing into a mortar and pestle.

2.3. VSM measurements

The magnetic moment as a function of applied field was measured for the prepared glasses on a VSM (Lakeshore VSM 7410) within the magnetic range ± 1.5 T with a time constant of 1 s and sensitivity $10^{-6.5}$ emu at RT.

2.4. EPR spectroscopy

EPR spectroscopy measurements were performed on an X-band EPR spectrometer (JEOL Model JES FA200) at X-band frequency (≈ 9.4 GHz) and a magnetic field modulation of 100 kHz. The microwave power of 1 mW was used for EPR measurements. The amplitude of the magnetic modulation was kept at about 1 mG (one milligauss) and the first derivative of the resonance absorption was obtained against the DC magnetic field sweep in the desired range. The suitable amounts of powdered glasses were filled in thin walled quartz capillary for the EPR experiment. The EPR spectrum of FVNB0 was also recorded at liquid nitrogen temperature (LNT) by dipping the sample in liquid nitrogen in a quartz cold-finger Dewar.

3. Results and discussion

3.1. XRD

All these samples examined by powder XRD at RT gave XRD patterns which were free from any sharp diffraction peaks. The patterns displayed only broad characteristic hump of glasses. The XRD results confirmed the amorphousness of the samples. The characteristic XRD patterns are shown in Fig. 1.

3.2. Magnetization

The representative magnetization curves are shown in Fig. 2. These curves indicate the paramagnetic nature of the glass samples under study due to the presence of the linear magnetization curves up to magnetic fields of cycle ± 15 kG (kilo gauss). The magnetic data for all the samples are given in Table I.

The magnetization in FVNB0 is only caused by vanadium as there is no iron in this sample. The magnetization curve cannot resolve the issue of existing oxidation states of vanadium or iron. In this regard, complementary information can be provided by EPR results. They confirm an assumption that the vanadium ion V^{4+} is the the main paramagnetic species in FVNB0. Therefore, the magnetization in these glasses is assigned mainly to V^{4+} , however, the measured value of magnetization indicates that only about 10.6% of the total vanadium exists in the (V^{4+}) magnetic state. A similar observation was reported by Mekki et al. in vanadium-sodium-silicate glasses where only 2% of the total vanadium was found in V^{4+} oxidation state and the

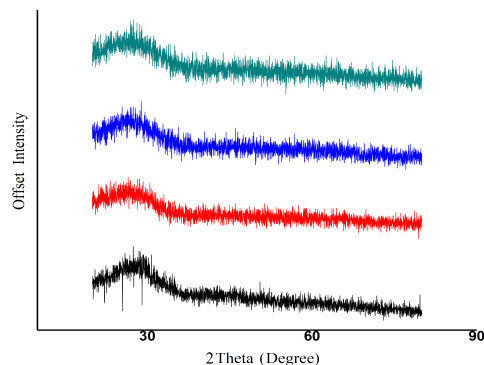


Fig. 1. XRD patterns of the FVNB x ($x = 0, 2, 3$ and 5) glasses recorded at RT: black — FVNB0, red — FVNB2, blue — FVNB3, green — FVNB5.

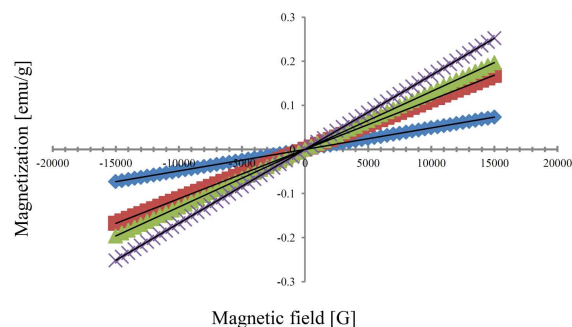


Fig. 2. The magnetograms of FVNB x glasses obtained with VSM at RT (\blacklozenge — $x = 0$, \blacksquare — $x = 2$, \blacktriangle — $x = 3$, \times — $x = 5$). Lines are the linear fits to the data.

rest of it remained in the non-magnetic V^{5+} oxidation state [14]. A similar result was reported in $2V_2O_5-38Li_2O-60P_2O_5$ glasses by Chand et al. [13] where only 12% of the total vanadium was estimated to be in magnetic V^{4+} oxidation state. Assuming, however, that all vanadium exists in a magnetic state V^{4+} , the reduced effective magnetization could be explained by means of a canted AFM pairing (CAFMP) of magnetic moments like $M_{\text{eff}} = M_A - M_B \cos(\varphi)$, where $M_A = M_B$ and φ is the angle between the paired magnetic moments M_A and M_B . The resultant M_{eff} per pair is the reduced magnetic moment of vanadium [13]. If the canting angle φ is close to zero, the resultant magnetic moment will also be close to zero. In the case of FVNB0, the canting angle is estimated to be 26.6° assuming a 100% V^{4+} oxidation state of the total vanadium. This means that two V^{4+} magnetic dipoles ($\mu = 1.7$ BM) are paired antiferromagnetically with a canting angle of $\approx 26.6^\circ$ resulting in an effective magnetic moment $\mu_{\text{eff}} = 0.18$ BM per pair.

The EPR study of FVNB0 glass is special since no iron is involved, hence the study will provide specific information about the oxidation states of vanadium in the sample. Detailed discussion will be presented later during the EPR analysis in Sect. 3.3.

TABLE I

The magnetization data of the FVNB x glasses. FM — formula mass, $M_{@15\text{ kG}}$ — magnetization at 15 kG, χ_m — molar susceptibility, $\mu_{\text{eff}/FU}$ — estimated effective magnetic moment per formula unit, $\mu_{\text{eff}/(V^{4+}\text{ or Fe}^{3+})}$ — estimated effective magnetic moment per V^{4+} or Fe^{3+} ion, $\mu_{\text{eff}/\text{pair}}$ — estimated μ_{eff} per CAFM pair and \emptyset — canted angle.

Sample	FM [g]	$M_{@15\text{ kG}}$ [emu/g]	χ_m [emu/(g mol)]	$\mu_{\text{eff}/FU}$ [BM]	$\mu_{\text{eff}/(V^{4+}\text{ or Fe}^{3+})}$ [BM]	$\mu_{\text{eff}/\text{pair}}$ [BM]	\emptyset [Degree]
FVNB0	10120	0.073	0.049	10.8	0.18	0.18 (V^{4+}) _{pair}	$\approx 26.6^\circ$
FVNB2	10076	0.168	0.113	16.3	1.56	1.56 (Fe^{3+}) _{pair}	$\approx 49.2^\circ$
FVNB3	10054	0.197	0.132	17.6	1.26	1.26 (Fe^{3+}) _{pair}	$\approx 43.9^\circ$
FVNB5	10010	0.252	0.168	19.9	1.09	1.09 (Fe^{3+}) _{pair}	$\approx 40.5^\circ$

However, at this stage it is enough to mention that either vanadium exists in majority in the non-magnetic V^{5+} oxidation state and V^{4+} oxidation state is in minority or there exists an AFM coupling between the V^{4+} sites similar to NaVO_3 [14]. From Table I it is clear that upon replacing V by Fe atoms, even by a small fraction, the magnetization increases by many folds. Its increase is anticipated by the fact that iron (both Fe^{2+} and Fe^{3+}) possesses a much higher magnetic moment ($\mu_{\text{eff}} \approx 4.5$ BM) in its high spin states as compared to V^{4+} ($\mu_{\text{eff}} \approx 1.7$ BM) which, in turn, is in low concentration. Therefore the magnetization of these glasses is mainly due to iron while vanadium makes a negligible contribution. In low spin state Fe^{2+} becomes diamagnetic while low spin Fe^{3+} has a single unpaired electron and its magnetic moment is equal to that of V^{4+} . EPR spectroscopic studies of these glasses indicate that iron surely exists in high spin Fe^{3+} oxidation state but about Fe^{2+} EPR is silent. Assuming the presence of only Fe^{3+} ions, the measured values of magnetization indicate that the effective magnetic moment per iron magnetic species is very much reduced (about by one order of magnitude) as compared to theoretical value (4.5 BM). Such reduction in effective magnetic moment of Fe^{3+} is possible by the earlier proposed CAFMP effect of iron magnetic moments [13].

The analysed data given in Table I clearly indicate that the reduction in the effective magnetic moment varies from sample to sample depending upon the x iron content. One can also observe that the μ_{eff} of Fe^{3+} is decreasing and, correspondingly, the proposed canting angle φ is decreasing as the content x of iron increases from 0 to 5. Due to the observed reduction of the magnetization, these glasses may be called dilute magnetic glasses. The linear part of the magnetization was used to calculate the $\chi = M/H$ and the variation of χ vs x is shown in Fig. 3.

3.3. EPR

The EPR spectra of the samples are shown in Figs. 4 and 5. The glass FVNB0 does not contain any iron. The EPR signals, therefore, should arise due to vanadium only. In diamagnetic hosts, sharp

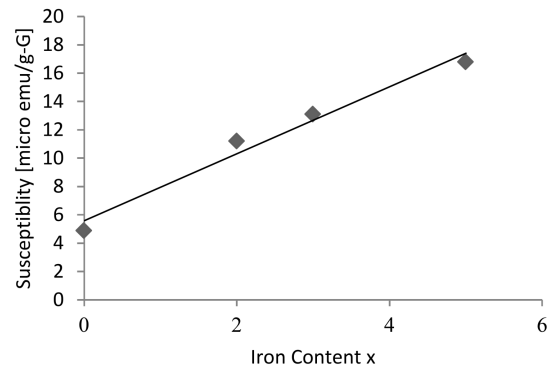


Fig. 3. The variation of susceptibility χ vs x in FVNB x ($x = 0, 2, 3$ and 5) glasses at RT. The line is a linear fit: $y = 2.36x + 5.58$ with $R^2 = 0.98$.

line EPR spectra of vanadium(IV) magnetic ions are observed even at RT due to the absence of magnetic dipolar broadening and super-exchange interactions [15]. Vanadium(IV) usually forms a distinct covalent bond with oxygen resulting in the vanadyl molecular ion $(V=O)^{2+}$ whose characteristic EPR spectrum ($S = 1/2, I = 7/2$ for ^{51}V) is easily identified by characteristic eight hyperfine lines due to nuclear spin $I = 7/2$. Vanadyl EPR can be easily identified in crystals, liquids, powders and glasses. In glasses, a characteristic sixteen line spectrum (a combination of $\theta = 0^\circ$ and $\theta = 90^\circ$, i.e., respectively, the so called perpendicular and parallel part) is shown by vanadyl ions when only moderate dipolar and/or exchange interactions are present (see Fig. 6) [13, 15]. A comparison of Figs. 4 and 6 clearly demonstrates the effect of strong magnetic exchange interactions on the EPR spectra of V^{4+} in the FVNB0 glass. The most important line broadening mechanisms in EPR are dipolar and super-exchange interactions.

The magnetic exchange interactions between like spins cause a narrowing of the EPR lines whereas the magnetic exchange interactions between unlike spins cause a broadening of the EPR lines [16, 20]. Broadening or smearing of EPR spectra may occur due to fast magnetic exchange interactions and/or motions of the ions [17]. As a consequence, liquids show an averaged eight hyperfine lines and in higher

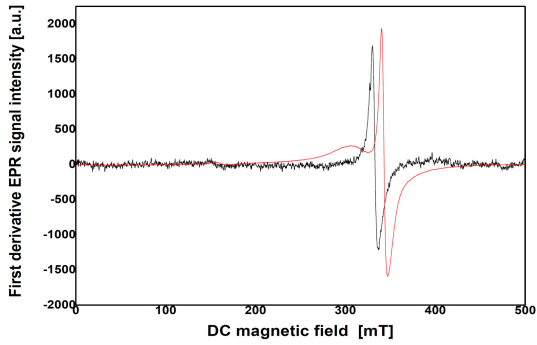


Fig. 4. X-band EPR spectra of the FVNB0 glass at RT (red) and at LNT (black) are compared to resolve the issue of low field minor signal between 100 mT and 200 mT.

concentrations of vanadium(IV) even the hyperfine structure is smeared out [16, 17, 21]. Contrary to this, a well resolved 8-line EPR spectrum was reported even for the pure vanadyl complex due to the reduced magnetic exchange and absence of dipolar broadening [21]. Since the V_2O_5 content in FVNB0 is high, i.e., meaning that 11% of total vanadium is estimated to be in the V^{4+} oxidation state, one expects the moderate magnetic exchange interaction in the EPR spectrum at RT, similar as in FVLP0 [13]. In turn, the smeared out hyperfine-structure in the EPR spectrum is less expected in FVNB0. Now, the EPR spectra of FVNB0 shown in Fig. 4 confirm the exchange narrowing both at RT and at LNT. The narrowing of the EPR signal at LNT, as compared to RT, indicates that the exchange interaction has become more rapid at LNT as compared to RT [16, 20]. The smeared EPR signals may be characterised by a parameter g (g -tensor) which is independent of the EPR spectrometer's operating frequency. It is defined as:

$$g = \frac{h\nu}{\beta B_{\text{reson}}} \quad (1)$$

where h is Planck's constant, ν is the EPR spectrometer's operating frequency, β is the Bohr magneton and B_{reson} is the resonance field (i.e., the center of the resonance peak in terms of the applied external magnetic field). The expression may be rewritten as

$$g = 71.448 \frac{\nu}{B_{\text{reson}}} \left[\frac{\text{GHz}}{\text{mT}} \right], \quad (2)$$

In the EPR spectrum of FVNB0 at RT (Fig. 4), there are three resonance signals at g values of 1.97, 1.99, and 4.16. The narrow and the prominent EPR signal at $g = 1.97$ with a peak to peak line width (ΔB_{pp}) of ≈ 6.8 mT is assigned to V^{4+} (vanadyl VO^{2+}) which occurred due to magnetic exchange narrowing in between like spins and is observed at an average g value called

$$g_{\text{iso}} = \frac{(g_x + g_y + g_z)}{3} \frac{(g_{\parallel} + 2g_{\perp})}{3}. \quad (3)$$

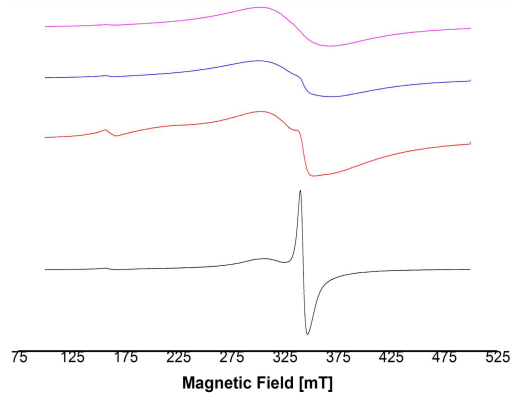


Fig. 5. EPR spectra of FVNB x at RT and at X-band in order of FVNB0, FVNB2, FVNB3 and FVNB5 from bottom to top. The y -axis represents the offset first derivative EPR signal intensities at different gains.

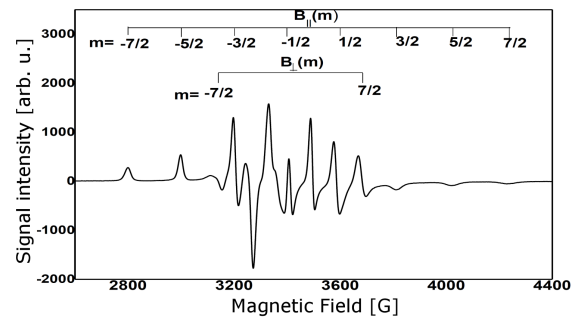


Fig. 6. Well-resolved sixteen line EPR spectrum of vanadyl species in FVLP0 glass at RT and X-band. The peaks of the parallel and perpendicular parts are identified by $B_{\parallel}(m)$ and $B_{\perp}(m)$ respectively, where m stands for the nuclear spin quantum number of vanadium. Figure 6 was taken from Ref. [13].

The other two subordinate EPR signals may result due to a small fraction of vanadium in either V^{3+} or V^{2+} oxidation state. In fact, V^{2+} is a relatively unstable oxidation state of vanadium — usually obtained by photoreduction of V^{3+} to V^{2+} . As V^{3+} is a non-Kramers ion with $S = 1$, hence with local symmetry less than octahedral (cubic) it will be usually EPR silent at X-band frequencies. This happens due to large zero field splitting (ZFS) parameter D which is greater than the X-band microwave quanta ($\approx 0.3 \text{ cm}^{-1}$) such that no spin allowed ($\Delta M_s = \pm 1$) EPR transitions are within the experimental frequency-magnetic field range [17, 22–25]. The allowed transitions occur when the following condition is satisfied:

$$h\nu = |D - \beta g_{\parallel} B|. \quad (4)$$

Therefore, these transitions depend on a ZFS parameter D and the operating EPR spectrometer frequency ν . In the FVNB0 glass, there are two EPR signals at RT (Fig. 4). There is one EPR signal at 338 mT with relatively broad line width ($\Delta B_{pp} \approx 63$ mT) which is assigned to the allowed

EPR Parameters of FVNBx glasses.

TABLE II

Sample	Signal	Freq. [MHz]	B_{reson} [mT]	ΔB_{pp} [mT]	g (± 0.01)	Remarks
FVNB0	1	9453.7	343.6	6.8	1.97	sharp
	2		338.5	63.0	1.99	broad
	3		162.5	11.0	4.16	weak
	LNT	9178.6	333.4	7.1	1.97	single
FVNB2	1	9452.2	327.5	50.0	2.06	broad
	2		161.7	9.5	4.17	weak
FVNB3	1	9452.3	335.2	67.3	2.01	broad
	2		161.8	8.8	4.17	weak
FVNB5	1	9452.0	334.5	67.0	2.02	broad
	2		160.3	8.1	4.21	weak

transition as per (2). The large line width is assigned mainly to the variation of ZFS parameter D at various V^{3+} sites in the glass matrix. The rough estimate reveals that the ZFS parameter D at RT is about 0.6 cm^{-1} . The hyperfine splitting is absent due to magnetic exchange interactions, as discussed earlier. However, a weak signal for ($\Delta M_s = 2$), which is normally forbidden, can also be seen in pseudo-octahedral local symmetry at

$$B_{\text{reson}} = \frac{h\nu}{2} \beta g_{\parallel}. \quad (5)$$

This transition is independent of the ZFS parameter D , thus it is only slightly broadened due to g_{\parallel} strain in the glass. Consequently, this EPR signal has usually been sharp. With $g_{\parallel} = 1.9$ for V^{3+} , such a signal is expected to appear at a magnetic field of $\approx 177.7 \text{ mT}$ at a frequency of 9.45 GHz . In Fig. 4, this signal is observed at $\approx 177 \text{ mT}$ with a peak-to-peak line width ΔB_{pp} of 11 mT . When the EPR is recorded at LNT, only the main line spectrum is observed which is assigned to V^{4+} , and the subordinate spectrum due to V^{3+} disappears. The reason seems to be due to the distortion of the local symmetry around V^{3+} and the consequent increase in the ZFS parameter D which makes the V^{3+} EPR silent at X-band within the magnetic field range of the experiment. It is thus concluded that out of the two magnetic oxidation states, V^{3+} and V^{4+} , in the FVNB0 glass, the latter state is in majority and the negligible fraction is in V^{3+} . The presence of traces of V^{3+} can be neglected for the estimation of magnetization. Therefore, for magnetization estimation only the V^{4+} oxidation state was considered in estimating the μ_{eff} for vanadium earlier in Sect. 3.2.

Now, we consider the EPR in the FVNB2, FVNB3 and FVNB5 glasses. Iron is one of the most pervasive impurities in borate and phosphate glasses. Notably, Fe^{2+} is EPR silent at RT. The ferric ion in the absence of external magnetic field has three Kramers doublets which split into six levels corresponding to M_S value from $+5/2$ to $-5/2$ and its EPR spectrum is expected to show five resonance signals according to allowed transitions

$\Delta M_S = \pm 1$ [17, 24]. The EPR spectrum of the ferric complex is described by the following spin Hamiltonian [17, 24]:

$$H = g\beta\mathbf{B} \cdot \mathbf{S} + D \left(S_z^2 + \frac{S(S+1)}{3} \right) + E(S_x^2 - S_y^2). \quad (6)$$

Here D and E are called the axial and tetragonal ZFS parameters, respectively, and S_i ($i = x, y, z$) denotes the components of spin \mathbf{S} . In the case of Fe^{3+} , it has an isotropic g -tensor (i.e., $g_x = g_y = g_z = 2$ is the free electronic value) but D and E depend on the local environment as well as are anisotropic. In regular octahedral local ligand field, both D and $E = 0$ and the EPR spectrum comprises a closely spaced quintet at $g = 2$. This quintet becomes a single broad line under the influence of dipolar broadening in systems having a higher concentration of iron. In local fields of lower symmetry (octahedral + tetragonal), the energy levels of Fe^{3+} in an external magnetic field become complicated if external magnetic field B is not along the principal axis. In a tetragonal microsymmetry $E = 0$ and if $D \gg h\nu$, only transitions between the $|\pm 1/2\rangle$ energy states will be observed at $g = 2$ ($g = g_{\parallel}$) for B parallel to z -axis of the ZFS tensor but for B_{\perp} to the z -axis of ZFS tensor the resonance signal will be observed at $g \approx 6$ ($= g_{\perp}$) [24–28]. Specific parameters of the EPR spectra are collated in Table II. Some specific features of the Fe^{3+} EPR, such as line width (ΔB_{pp}) and line shape in glass matrices, depend on the glass composition and the concentration of paramagnetic ions.

The EPR spectra of most glasses containing iron exhibit the two well-known resonances at the effective g values ($g_{\text{eff}} \approx 2$ and $g_{\text{eff}} \approx 30/7$) that have been considered as a signature of the presence of Fe^{3+} ions in a glassy host. The X-band (frequency $\approx 9 \text{ GHz}$) EPR spectra of most oxide glasses with low Fe^{3+} concentrations show an EPR signal at $g_{\text{eff}} = 30/7$ which is relatively narrow, and in most of the cases a broader EPR signal at $g_{\text{eff}} = 2$ is also observed even at RT. McGavin and Tennant [26] have explained in detail the occurrence

of an isotropic g -tensor in high spin d^5 systems under various conditions for D and E . The observation of an intense isotropic signal at $g \approx 30/7$ and a weak signal at $g \approx 9.7$ may generally be taken to be indicative of high spin Fe^{3+} in a rhombic environment ($D = 3E$). It has been discussed by Golding et al. [27] that both tetragonal and rhombic distortions from octahedral symmetry may give isotropic signal $g \approx 30/7$ under different conditions. Iwamoto et al. [28] have investigated the state of Fe^{3+} ion and $\text{Fe}^{3+}\text{-F}^-$ interaction in $x\text{CaF}_2\text{-}9(1-x)\text{CaO-}9\text{SiO}_2$ ($0 \lesssim x < 0.3$) glasses by EPR and similarly observed two resonances near $g = 2.0$ and $g = 4.3$ which were assigned to Fe^{3+} ions with dipole-dipole interactions and isolated Fe^{3+} ions in rhombic symmetry, respectively [28]. A careful look at the EPR parameters of FVNB2, FVNB3 and FVNB5 given in Table II reveals that only two EPR signals are prominently due to Fe^{3+} and lie at $g_{\text{eff}} \approx 2$ and $g_{\text{eff}} \approx 30/7$. The $g_{\text{eff}} \approx 2$ EPR signal is broad due to magnetic exchange interactions and the $g_{\text{eff}} \approx 30/7$ is narrow but weak. These features may be explained by the two different types of Fe^{3+} co-ordinations with oxygens: distorted octahedral and distorted tetragonal. The distorted iron site co-ordinations causing very large zero field splitting D and the magnetic exchange interactions (dipolar as well as super-exchange) manifest in the observed EPR characteristics of these glasses.

4. Conclusions

The magnetic study of dilute magnetic glasses $40\text{B}_2\text{O}_3 + 30\text{Na}_2\text{O} + (30 - x)\text{V}_2\text{O}_5 + x\text{Fe}_2\text{O}_3$ with $x = 0, \dots, 5$ has been undertaken to understand the effect of magnetic interactions and super-exchange between like and unlike spins by the methods of magnetization measurement and EPR spectroscopy. The following outcomes may be highlighted:

1. Only about 11% of the total vanadium existed in V^{4+} which is similar to the observation in the $2\text{V}_2\text{O}_5\text{-}38\text{Li}_2\text{O-}60\text{P}_2\text{O}_5$ glasses [13] where vanadium content was far less as compared to the FVNB x glasses under study. The contribution of vanadium to the magnetic moment of FVNB x glasses is minor despite vanadium being in much higher concentrations as compared to FVLP x glasses.
2. EPR confirms the presence of vanadium in V^{4+} oxidation state and iron in Fe^{3+} oxidation state in these glasses. Sodium appears to play a role in keeping the concentration of V^{4+} low in the glass networks of FVNB x glasses.
3. Despite being in minority, the concentration of V^{4+} is found sufficient to cause magnetic exchange effects on the EPR spectra of both vanadium and iron.
4. The major contribution to the magnetization of these glasses comes from iron. The effective magnetization is found much reduced from the

expected one. A CAFMP is suggested for the reduction of the experimental magnetization. Despite having high concentrations of vanadium and iron these glasses are found to be magnetically dilute.

5. The EPR spectra are affected by magnetic exchange interactions as well as by dipolar broadening due to like and unlike magnetic dipoles. A negligible presence of V^{3+} is also indicated by EPR in FVNB0.
6. The iron is concluded to exist in high spin Fe^{3+} spin state. The EPR spectra reveal that iron is surrounded by highly distorted pseudo-octahedral oxygen environments in the FVLB x ($x = 2, 3, 5$) glass networks. This causes very high rhombicity ($E/D \approx 0.3$) in the iron co-ordination. The EPR spectra of iron are further manipulated by the existence of super-exchange interactions between like and unlike spins V^{4+} and Fe^{3+} .

Acknowledgments

The authors are thankful to Professor S.K. Khasa, Department of Physics, Deenbandhu Chotu Ram University of Science and Technology (DCRUST), Murthal, Sonapat, India for the rendered help, many valuable discussions and suggestions.

References

- [1] N.P. Bansal, R.H. Doremus, *Handbook of Glass Properties*, Academic Press (Indian Reprint), 2006.
- [2] D.L. Griscom, *Borate Glasses: Structure, Properties and Applications*, Plenum, New York 1978.
- [3] H. Scholze, *Glass: Nature, Structure and Properties*, Springer, New York 1991.
- [4] M.S. Gaffar, F.H. El-Batal, M. El-Gazery, S.A. Mansaur, *Acta Phys. Pol. A* **115**, 671 (2009).
- [5] N. Guskos, G. Zolnierkiewicz, M. Pilarska, J. Typek, A. Blonska-Tabero, C. Aidinis, *Acta Phys. Pol. A* **132**, 24 (2017).
- [6] S. Gu, Z. Wang, S. Jiang, H. Lin, *Ceram. Int.* **40**, 7643 (2014).
- [7] N. Laorodphan, P. Pooddee, P. Kidkhunthod, P. Kunthadee, W. Tapala, R. Puntharod *J. Non-Cryst. Solids* **453**, 118 (2016).
- [8] I. Kashif, S.A. Rahman, A.A. Soliman, E.M. Ibrahim, E.K.A. Khalek, A.G. Mostafa, A.M. Sanad, *Physica B* **404**, 3842 (2009).
- [9] V. Naresh, S. Buddhudu, *Ferroelectrics* **437**, 110 (2012).

- [10] *Advances in Non-Crystalline Solids: Metallic Glass Formation, Magnetic Properties and Amorphous Carbon Films*, Eds. H. Montiel, G. Alvarez, Transworld Research Network, Trivandrum (India) 2010, Ch. 7.
- [11] I. Ardelean, M. Peteanu, S. Filip, V. Simon, I. Todor, *Solid State Commun.* **105**, 339 (1998) and references therein.
- [12] R. Stefan, M. Karabulut, *J. Mol. Struct.* **1071**, 45 (2014).
- [13] P. Chand, L. Kumar, S. Khasa, *Acta Phys. Pol. A* **137**, 1196 (2020).
- [14] A. Mekki, G.D. Khattak, D. Holland, M. Chinkhota, L.E. Wenger, *J. Non-Cryst. Solids* **318**, 193 (2003).
- [15] P. Chand, V.K. Jain, G.C. Upreti, *Magn. Reson. Rev.* **14**, 49 (1988).
- [16] G.C. Upreti, R.S. Saraswat, *Magn. Reson. Rev.* **7**, 215 (1982).
- [17] J.A. Weil, J.R. Bolton, J.E. Wertz, *Electron Paramagnetic Resonance: Elementary Theory and Practical Applications*, Wiley, 1994.
- [18] D. Jiles, *Introduction to Magnetism and Magnetic Materials*, CRC Press, 2015.
- [19] P. Chand, R. Chand Srivastava, A. Upadhyay *J. Alloys Compd.* **460**, 108 (2008).
- [20] J.H. Van Vleck, *Phys. Rev.* **74**, 1168 (1948).
- [21] S. Sharma, A. Kumar, P. Chand, B.K. Sharma, S. Sarkar, *Spectrochim. Acta A* **63**, 556 (2006).
- [22] P.J. Alonso, J. Forniés, M.A. García-Monforte, A. Martín, B. Menjón, *Chem. Commun.* **20**, 2138 (2001).
- [23] J. Krzystek, A.T. Fiedler, J.J. Sokol, A. Ozarowski, S.A. Zvyagin, T.C. Brunold, J.R. Long, L.-C. Brunel, J. Telsler, *Inorg. Chem.* **43**, 5645 (2004).
- [24] J.W. Orton, *Electron Paramagnetic Resonance*, Illife Books, London 1968, Chs. 5 and 11.
- [25] J. Ashkin, N.S. Vandervan, *Physica B+C* **95**, 1 (1978).
- [26] D.G. McGavin, W.C. Tennant, *Mol. Phys.* **45**, 77 (1982).
- [27] R.M. Golding, M. Kestigian, W.C. Tennant, *J. Phys. C Solid State Phys.* **11**, 5041 (1978).
- [28] N. Iwamoto, Y. Makino, S. Kasaha, *J. Non-Cryst. Solids* **55**, 113 (1983).